第 36 卷第 3 期
2020 年 3 月

无 机 化 学 学 报
CHINESE JOURNAL OF INORGANIC CHEMISTRY

Vol.36 No.3
503-514

基于香豆素 Schiff 碱双核 Ni(Ⅱ)和立方烷型 $Cu_4(\mu_3\text{-}O)_4$ 的四核 Cu(Ⅱ)配合物的合成、晶体结构及光谱性质

张淑珍[1] 常 健[1] 张宏佳[1] 武 娅[1] 孙银霞*,[1] 王彦斌[2]

([1]兰州交通大学化学与生物工程学院,兰州 730070)

([2]西北民族大学化工学院,甘肃省高校环境友好复合材料及生物质利用重点实验室,兰州 730070)

摘要:合成了 2 个 3-氨基-4-羟基香豆素类 Schiff 碱双核 Ni(Ⅱ)和立方烷型 $Cu_4(\mu_3\text{-}O)_4$ 的四核 Cu(Ⅱ)配合物,$[Ni(L^1)(DMF)(H_2O)]_2$ (**1**)(H_2L^1=3-((5-溴-2-羟基-亚苄基)-氨基)-4-羟基-苯并吡喃-2-酮)和$[Cu_4(L^2)_4]\cdot DMF\cdot CH_3OH\cdot 2H_2O$ (**2**)(H_2L^2=4-羟基-3-((2-羟基-3-甲氧基-亚苄基)-氨基)-苯并吡喃-2-酮),并通过元素分析、红外光谱、紫外光谱、荧光光谱及 X 射线单晶衍射分析等手段进行了表征。X 射线单晶衍射分析结果表明:配合物 **1** 具有双核结构,由 2 个金属离子和 2 个配体单元组成,配合物 **2** 具有立方烷型 $Cu_4(\mu_3\text{-}O)_4$ 的四核结构,由 4 个金属离子和 4 个配体单元组成。配合物 **1** 是单斜晶系、*C*2/*c* 空间群;配合物 **2** 是四方晶系,$I4_1/a$ 空间群,且中心金属 Ni(Ⅱ)和 Cu(Ⅱ)离子的空间构型均为六配位的扭曲的八面体。此外,配合物 **1** 通过分子间氢键、C–H$\cdots\pi$ 及 $\pi\cdots\pi$ 作用形成 1D 超分子链结构,配合物 **2** 通过分子内氢键和 $\pi\cdots\pi$ 作用形成 3D 超分子结构。此外,研究了 H_2L^1,H_2L^2 及其相应的 Ni(Ⅱ)和 Cu(Ⅱ)配合物的荧光性质。

关键词:香豆素 Schiff 碱;过渡金属配合物;晶体结构;光谱性质

中图分类号:O614.121 **文献标识码**:A **文章编号**:1001-4861(2020)03-0503-12

DOI:10.11862/CJIC.2020.056

Synthesis, Crystal Structure and Spectral Properties of Binuclear Ni(Ⅱ) and Cubane-like $Cu_4(\mu_3\text{-}O)_4$ Cored Tetranuclear Cu(Ⅱ) Complexes Based on Coumarin Schiff Base

ZHANG Shu-Zhen[1] CHANG Jian[1] ZHANG Hong-Jia[1] WU Ya[1] SUN Yin-Xia*,[1] WANG Yan-Bin[2]

([1]*School of Chemical and Biological Engineering, Lanzhou Jiaotong University, Lanzhou* 730070, *China*)

([2]*Northwest Minzu University, College of Chemical Engineering; Key Laboratory for Utility of Environment-friendly Composite Materials and Biomass in Universities of Gansu Province, Lanzhou* 730030, *China*)

Abstract: Dinuclear Ni(Ⅱ) and cubane-like $Cu_4(\mu_3\text{-}O)_4$ cored tetranuclear Cu(Ⅱ) complexes, $[Ni(L^1)(DMF)(H_2O)]_2$ (**1**) (H_2L^1=3-((5-bromo-2-hydroxy-benzylidene)-amino)-4-hydroxy-benzopyran-2-one), $[Cu_4(L^2)_4]\cdot DMF\cdot CH_3OH\cdot 2H_2O$ (**2**) (H_2L^2 =4-hydroxy-3-((2-hydroxy-3-methoxy-benzylidene)-amino)-benzopyran-2-one) based on 3-amino-4-hydroxy-coumarin Schiff base ligands were synthesized and characterized by elemental analysis, IR, UV-Vis, emission spectra and X-ray single crystal diffraction analysis. The X-ray single crystal diffraction analysis results show that complex **1** has a binuclear structure composed of two metal ions and two ligand units, and complex **2** has a tetranuclear structure composed of four metal ions and four ligand units. Complex **1** crystallizes in monoclinic system, *C*2/*c* space group, whereas complex **2** crystallizes in tetragonal system, $I4_1/a$ space group. The spatial configurations of the central metal Ni(Ⅱ) and Cu(Ⅱ) ions are all six-coordinated distorted octahedron in complexes **1** and **2**, respectively. In addition, complex **1** forms a one-dimensional (1D) supramolecular chain through

收稿日期:2019-06-18。收修改稿日期:2019-11-14。

甘肃省重点研发计划项目(No.18YF1GA054),兰州交通大学优秀科研平台(No.201706)和甘肃省高校环境友好复合材料及生物质利用重点实验室开放课题资助项目。

*通信联系人。E-mail:sun_yinxia@163.com;会员登记号:02M100427534。

intermolecular hydrogen bonding, C–H⋯π and π⋯π stacking interactions, while complex **2** formed three-dimensional (3D) supramolecular network structure via intramolecular hydrogen bonding and π⋯π stacking interactions. CCDC: 1922258, **1**; 1922309, **2**.

Keywords: coumarin Schiff-base; transition metal complex; crystal structure; spectral property

0 Introduction

Schiff base compounds and their transition metal complexes are playing an important part in the development of coordination chemistry[1-5] because of their potential application in catalysis[6], bioscience[7-11], magnetic materials[12-17], luminescent[18-24], electrochemical systems[25-26] and constructing supramolecular structures building[27-33]. Schiff-base compounds and its derivatives are very important as versatile ligands, properties of interest in materials science. Also, the Schiff base ligands with N- and O- group are strong donors and therefore the oxime-containing ligands were found to efficiently stabilize high oxidation states of metal ions and prepare complexes with different structures and functionalities like Cu(Ⅱ) and Ni(Ⅱ) complexes[34-39]. In recent years, there has been enhanced interest in the synthesis and characterization of such complexes due to their interesting properties and other applications[40-47]. In order to further study the supramolecular of transition metal complexes and Schiff base ligands, we synthesized and analyzed two complexes, $[Ni(L^1)(DMF)(H_2O)]_2$ (**1**) (H_2L^1=3-((5-bromo-2-hydroxy-benzylidene)-amino)-4-hydroxy-benzopyran-2-one) and $[Cu_4(L^2)_4]\cdot DMF\cdot CH_3OH\cdot 2H_2O$ (**2**) (H_2L^2=4-hydroxy-3-((2-hydroxy-3-methoxy-benzylidene)-amino)-benzopyran-2-one). Complex **1** is a dinuclear structure and is connected to a 1D supramolecular chain by intermolecular hydrogen bonding, C–H⋯π and π⋯π stacking interactions. Complex **2** is a cubane-like $Cu_4(\mu_3\text{-}O)_4$ cored tetranuclear structure and is linked to a 3D network supramolecular structure by intramolecular hydrogen bonding and π⋯π stacking interactions. The central metal Ni(Ⅱ) and Cu(Ⅱ) ions are all six-coordinated distorted octahedron geometries in complexes **1** and **2**, respectively. In addition, the fluorescent properties of the ligands H_2L^1, H_2L^2 and their Ni(Ⅱ) complex **1** and Cu(Ⅱ) complex **2** are also studied.

1 Experimental

1.1 Materials

4-Hydroxyl coumarin from Alfa Aesar was used without further purification. The other reagents and solvents were of analytical grade from Tianjin Chemical Reagent Factory, and were used without further purification.

1.2 Instruments and methods

C, H and N analyses were carried out with a GmbH Vario EL V3.00 automatic elemental analyzer. FT-IR spectra were recorded on a VERTEX70 FT-IR spectrophotometer, with samples prepared as KBr (400~4 000 cm^{-1}) pellets. UV-Vis absorption spectra were recorded on a Hitachi UV-3900 spectrometer. Luminescence spectra in solution were recorded on a Hitachi F-7000 spectrometer. X-ray single crystal structure was determined on a Bruker Smart 1000 CCD area detector. Melting points were measured by an X-4 microscopic melting point apparatus made by Beijing Taike Instrument Limited Company and were uncorrected. ^1H NMR spectra were recorded in DMSO-d_6 solution at room temperature on a Bruker AV instrument operating at a frequency of 500 MHz and referenced to tetramethylsilane (δ=0.00) as an internal standard. Chemical shift multiplicities are reported as s=singlet, d=doublet, t=triplet and m=multiplet.

1.3 Syntheses of ligands H_2L^1 and H_2L^2

H_2L^1 and H_2L^2 were synthesized according to the following synthetic routes shown in Scheme 1.

1.3.1 Synthesis of 3-amino-4-hydroxycoumarin

3-Amino-4-hydroxycoumarin was synthesized according to an analogous method reported earlier[48]. Firstly, 0.9 mL concentrated HNO_3 and 1.8 mL

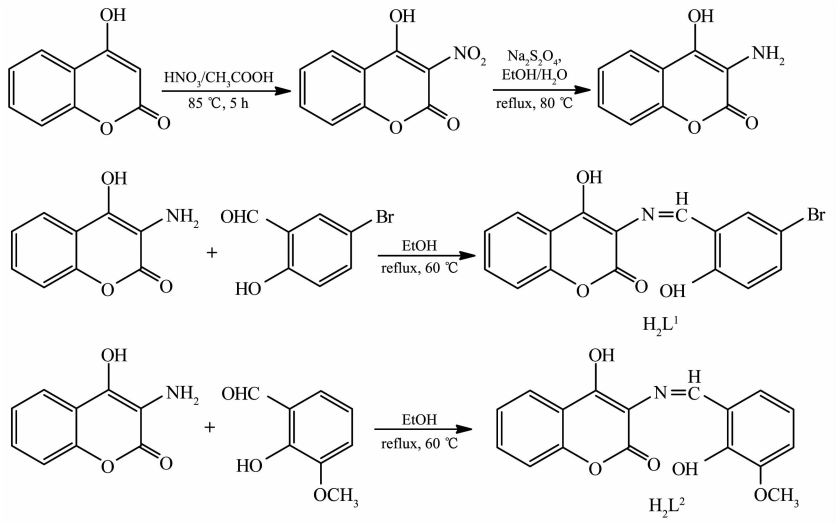

Scheme 1　Synthetic routes of H_2L^1 and H_2L^2

CH_3COOH mixed solution was added dropwise into the 4-hydroxycoumarin (20.5 g, 12.6 mmol) solution containing 5 mL glacial acetic acid over 0.5 h at 85 ℃, and the mixture was subjected to heating at 80 ℃ for 4 h. The mixed solution was allowed to come to room temperature, and placed in an ice-water mixture until a pale yellow solid appeared, which was filtered to give the 3-nitro-4-hydroxycoumarin. Secondly, $Na_2S_2O_4$ solid (33.0 g, 18.3 mmol) was added in batches to a solution of 3-nitro-4-hydroxycoumarin (10.0 g, 4.8 mmol) in EtOH/H_2O (2∶1, *V*/*V*) mixture solution (60 mL) at 87 ℃, and the reaction continued for 7 h. Then the ethanol was removed via vacuum distillation. The residual $Na_2S_2O_4$ was removed by reaction with concentrated hydrochloric acid, and neutralized with saturated sodium bicarbonate solution. The product was suction filtered and dried to give a brown 3-amino-4-hydroxycoumarin powder. Yield: 67.8%. m.p. 209~211 ℃. Anal. Calcd. for $C_9H_7NO_3$ (%): C, 61.02; H, 3.98; N,7.91. Found(%): C, 61.26; H, 3.67; N,7.72.

1.3.2　Synthesis of H_2L^1

3-Amino-4-hydroxycoumarin (177.0 mg, 1.0 mmol) and 2-hydroxy-5-bromobenzaldehyde (201.21 mg, 1.0 mmol) were placed in a 20 mL flask, and 7 mL of absolute ethanol was added to the flask. The mixture was subjected to reflux at 70 ℃ for 8 h, and allowed to come to room temperature. The light yellow precipitate was filtered and dried to obtain 267.79 mg H_2L^1. Yield: 61.07%. m.p.>300 ℃. Anal. Calcd. for $C_{16}H_{10}BrNO_4$ (%): C, 53.36; H, 2.80; N, 3.89. Found (%): C, 53.43; H, 2.74; N, 3.79. ^{1}H NMR (500 MHz, DMSO-d_6): δ 6.99 (d, *J*=9.0 Hz, 1H, Ph), 7.24 (td, *J*= 6.5,1 Hz, 1H, Ph), 7.33 (m, 2H, Ph), 7.62 (m, 2H, Ph), 7.79 (dd, *J*=3.5 Hz, 1H, Ph), 8.07 (s, 1H, CH=N), 9.86 (s, 1H, OH),10.99 (s, 1H, OH).

1.3.3　Synthesis of H_2L^2

The ligand H_2L^2 was synthesized by a method similar to that of H_2L^1 except substituting 2-hydroxy-5-bromobenzaldehyde with 2-hydroxy-3-methoxybenzaldehyde. H_2L^2: 193.21 mg, Yield: 62.23%. m.p. 247~249 ℃. Anal. Calcd. for $C_{17}H_{13}NO_5$(%): C, 65.59; H, 4.21; N,4.50. Found(%): C, 65.43; H, 4.35; N, 4.72. ^{1}H NMR (500 MHz, DMSO-d_6): δ 3.86 (t, *J*=14.5 Hz, 3H, OCH_3), 6.97 (t, *J*=14.5 Hz, 1H, Ph), 7.08 (s, 1H, Ph), 7.00 (s, 1H, Ph), 7.22 (m, 2H, Ph), 7.4 (s, 1H, Ph), 7.69 (td, *J*=12.5, 6.5 Hz, 1H, Ph),7.96 (dd, *J*=2,0 Hz, 1H, CH=N), 9.91 (s, 1H, OH),10.27 (s, 1H, OH).

1.4　Syntheses of complexes 1 and 2

A solution of Ni(Ⅱ) acetate monohydrate (2.48 mg, 0.01 mmol) in methanol (1 mL) was added dropwise to a solution of H_2L^1 (3.6 mg, 0.01 mmol) in acetone/DMF (7 mL, 6∶1, *V*/*V*). The color of the mixture turned to yellow immediately, and then 2 drops of triethylamine were added in it. The mixture was stirred for 1 h at room temperature, filtered, and the filtrate was allowed to stand at room temperature for about two weeks. The solvent was partially evaporated, and pale

yellow needle-like single crystals of complex **1** suitable for X-ray crystallographic analysis were obtained. Anal. Calcd. for $C_{38}H_{34}Br_2N_4Ni_2O_{12}$(%): C, 49.43; H, 3.37; N, 5.52. Found(%): C, 49.22; H, 3.75; N, 5.62.

The synthesis of Cu(Ⅱ) complex **2** was same as above to obtain yellow needle-like single crystals suitable for X-ray crystallographic analysis. Anal. Calcd. for $C_{72}H_{59}Cu_4N_5O_{24}$(%): C, 52.97; H, 3.64; N, 4.29. Found(%): C, 53.20; H, 3.40; N, 4.51.

1.5 Crystal structure determinations of complexes 1 and 2

The single crystals with approximate dimensions of 0.22 mm×0.26 mm×0.28 mm (**1**) and 0.22 mm×0.25 mm×0.27 mm (**2**) were placed on a Bruker Smart 1000 CCD area detector. The reflections were collected using graphite-monochromatized Mo $K\alpha$ radiation (λ = 0.071 073 nm) at 296(1) K and 296(2) K, respectively. The Lp corrections were applied to the SAINT program[49] and semi-empirical correction were applied to the SADABS program[50]. The crystal structures were solved by the direct methods (SHELXS-2014)[51]. Details of the crystal parameters, data collection and refinements for complexes **1** and **2** are summarized in Table 1.

CCDC: 1922258, **1**; 1922309, **2**.

Table 1 Crystal data and structure refinement for complexes 1 and 2

Complex	1	2
Empirical formula	$C_{38}H_{34}Br_2N_4Ni_2O_{12}$	$C_{72}H_{59}Cu_4N_5O_{24}$
Formula weight	1 015.87	1 491.27
Crystal system	Monoclinic	Tetragonal
Space group	*C*2/*c*	$I4_1/a$
a / nm	1.799 3(4)	1.663 3(4)
b / nm	0.921 0(2)	1.663 3(4)
c / nm	2.496 9(6)	2.342 9(4)
β / (°)	110.249(2)	
V / nm^3	3.881 8(2)	6.482(3)
Z	4	4
μ / mm^{-1}	3.098	1.374
F(000)	2 048	3 024
θ range / (°)	1.70~25.0	2.5~25.0
Limiting indices	$-21 \leqslant h \leqslant 19, -10 \leqslant k \leqslant 10, -29 \leqslant l \leqslant 29$	$-18 \leqslant h \leqslant 19, -19 \leqslant k \leqslant 18, -27 \leqslant l \leqslant 27$
Reflection collected, unique	14 365, 3 413 (R_{int}=0.174)	20 340, 2 862 (R_{int}=0.072)
Completeness to θ / %	100	99.9
Data, restraint, parameter	3 413, 0, 263	2 862, 0, 218
GOF on F^2	1.07	1.06
R_1, wR_2 [$I>2\sigma(I)$]	0.044 4, 0.108 31	0.039 6, 0.100 2
Largest diff. peak and hole / (e·nm^{-3})	820 and −810	860 and −890

2 Results and discussion

2.1 Crystal structures of complexes 1 and 2

The molecular structure of complexes **1** and **2** are shown in Fig.1 and 2, respectively, and selected bond lengths and angles are listed in Table 2. X-ray crystallographic analysis shows that complex **1** crystallizes in the monoclinic system, and the space group is *C*2/*c*. Complex **1** can be described as a binuclear Ni(Ⅱ) complex, consisting of two Ni(Ⅱ) ions, two $(L^1)^{2-}$ units and two coordinated solvent molecules H_2O and DMF. In complex **1**, two deprotonated hydroxyl oxygen (O3, O4) atoms and one oxime nitrogen (N1) atoms come from the $(L^1)^{2-}$ unit, as well as two oxygen (O5, O6) atoms of the coordinated solvent molecules H_2O and DMF, respectively, which constitute the $[Ni(L^1)(H_2O)(DMF)]$ moiety. And then the O4 and O4a atoms bridge the two $[Ni(L^1)(H_2O)(DMF)]$ moieties to form the binuclear structure $[Ni(L^1)(H_2O)(DMF)]_2$ (**1**). Thus, the central Ni(Ⅱ) ions are hexa-coordinated and

their coordination sphere is best described as a slightly distorted octahedron.

Complex **2** crystallizes in the tetragonal system, and the space group was $I4_1/a$. Complex **2** can be described as a cubane-like $Cu_4(\mu_3\text{-}O)_4$ cored tetranuclear Cu(Ⅱ) complex, and consist of four Cu(Ⅱ) ions and four $(L^2)^{2-}$ units, in which the ligand $(L^2)^{2-}$ is both chelating and bridging after double deprotonation of

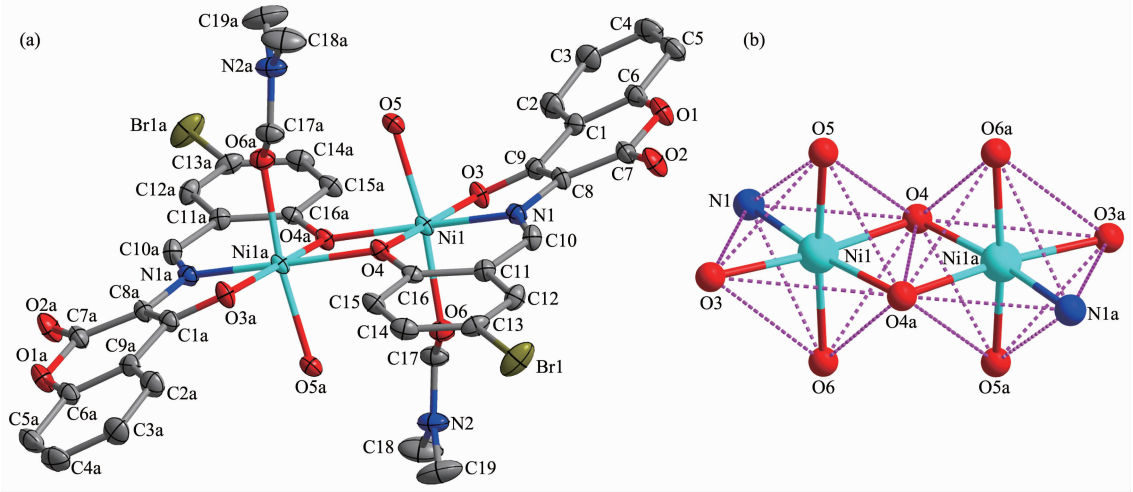

Symmetry code: a: 3/2−*x*, 3/2−*y*, 1−*z*

Fig.1　(a) Molecular structure of complex **1** showing 30% probability displacement ellipsoids; (b) Coordination pattern diagram for Ni(Ⅱ) ions of complex **1**

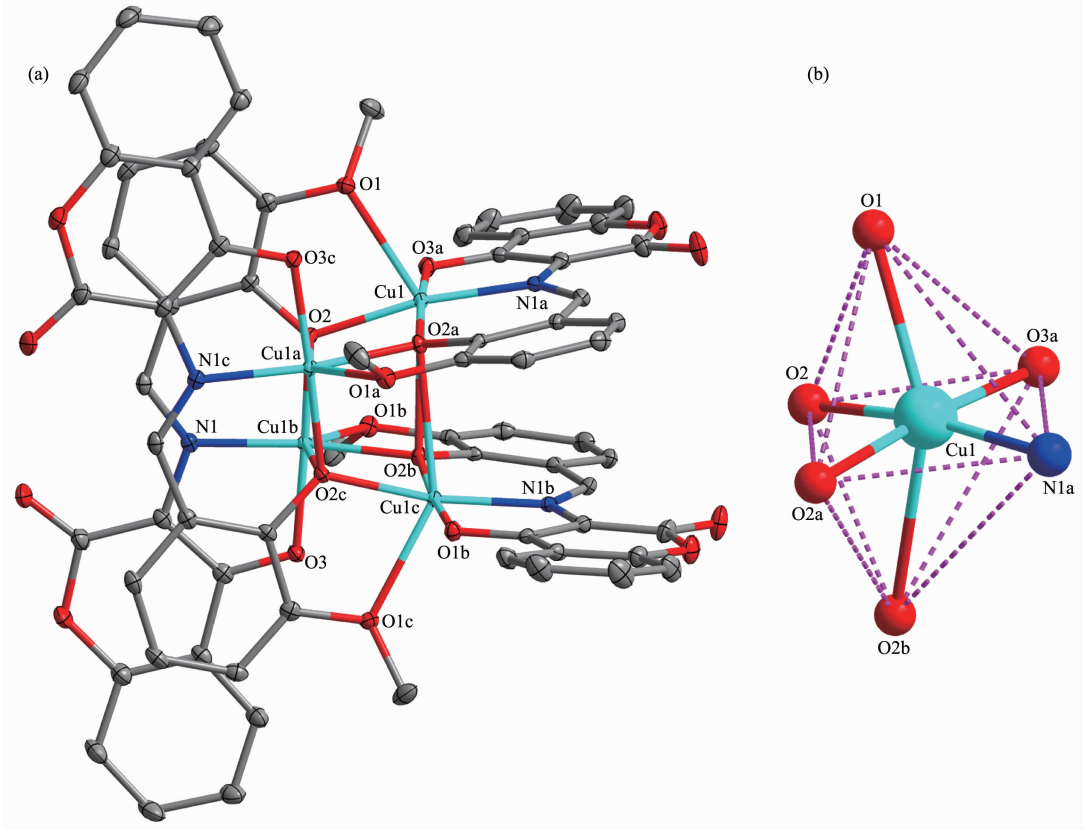

Symmetry codes: a: 3/4+*x*, 3/4−*y*, 3/4−*z*; b: 3/4−*x*, −3/4+*y*, 3/4−*z*; c: −*x*, 3/2+*y*, *z*

Fig.2　(a) Molecular structure of complex **2** showing 30% probability displacement ellipsoids; (b) Coordination pattern diagram for Cu(Ⅱ) ions of complex **2**

the phenolic hydroxyls. A [Cu(L^2)] moiety was constituted by two deprotonated hydroxyl oxygen (O2, O3) atoms, one oxime nitrogen (N1) atoms from one of the ligand units (L^2)$^{2-}$, and the oxygen (O1) atom of the methoxy group coming from this (L^2)$^{2-}$ units coordinated to the adjacent [Cu(L^2)] moiety (Fig.3a). By self-assembly, four such monomeric [Cu(L^2)] entities eventually are linked through alkoxo (O2 and O2a) bridges to produce the tetranuclear cubane Cu$_4$(μ_3-O)$_4$ core. This Cu$_4$(μ_3-O)$_4$ core consists of four alkoxo-bridged Cu(Ⅱ) centers approximately arranged in a cuboid geometry of an alternating array of Cu and O atoms that occupy the corners of the cube (Fig.3b). This structure could alternatively be seen as two interpenetrated Cu$_4$ and O$_4$ tetrahedrons. The four pincer ligands (L^2)$^{2-}$ are all in the binding mode μ_3-η^1:

Table 2 Selected bond lengths(nm) and bond angles(°) for complexes 1 and 2

			1		
Ni1-O3	0.205 0(2)	Ni1-O4	0.201 6(3)	Ni1-O5	0.208 4(2)
Ni1-O6	0.210 0(2)	Ni1-N1	0.201 2(3)	Ni1-O4a	0.206 4(2)
O3-Ni1-O4	172.93(8)	O3-Ni1-O5	87.32(7)	O3-Ni1-O6	93.89(8)
O1-Ni1-N1	82.01(8)	O1-Ni1-O4a	105.58(8)	O4-Ni1-O5	90.81(7)
O4-Ni1-O6	88.92(7)	O4-Ni1-N1	91.42(9)	O4-Ni1-O4a	80.95(8)
O5-Ni1-O6	171.90(9)	O5-Ni1-N1	96.12(8)	O5-Ni1-O4a	83.42(8)
O6-Ni1-N1	91.99(9)	O6-Ni1-O4a	88.54(8)	N1-Ni1-O4a	172.34(8)
			2		
Cu1-O1	0.234 7(2)	Cu1-O2	0.198 5(2)	Cu1-O2a	0.196 1(2)
Cu1-O3a	0.194 5(2)	Cu1-N1a	0.195 1(2)	Cu1b-O2	0.196 1(2)
Cu1b-O3	0.194 5(2)	Cu1b-N1	0.195 1(2)	Cu1-O2b	0.268 2(2)
O1-Cu1-O2	75.51(7)	O1-Cu1-O2a	100.98(7)	O2-Cu1-O2a	88.76(8)
O1-Cu1-O3a	84.41(7)	O2-Cu1-O3a	91.75(7)	O2A-Cu1-O3a	174.54(7)
O3A-Cu1-N1a	85.16(8)	O1-Cu1-N1a	114.44(7)	O2-Cu1-N1a	169.13(8)
O2A-Cu1-N1a	93.35(8)	Cu1-O2-Cu1b	111.26(8)		

Symmetry codes: a: 3/2–x, 3/2–y, 1–z for **1**; a: 3/4+x, 3/4–y, 3/4–z; b: 3/4–x, –3/4+y, 3/4–z for **2**.

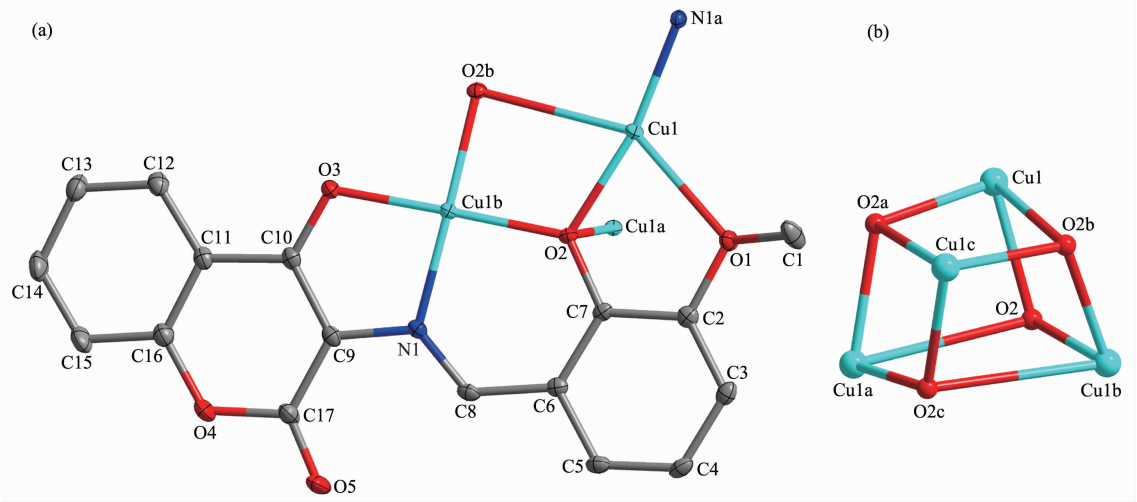

Symmetry codes: a: 3/4+x, 3/4–y, 3/4–z; b: 3/4–x, –3/4+y, 3/4–z; c: –x, 3/2+y, z

Fig.3 (a) Structure of [Cu(L^2)] moiety of complex **2** showing 30% probability displacement ellipsoids; (b) Distorted Cu$_4$O$_4$ core of the cubane-like isomer (30% probability ellipsoids) with no crystallographic constraint

η^1:η^3, and all four bridging alkoxo oxygens are located at the four corners of the cube, each bridging three Cu(Ⅱ) ions. Four Cu(Ⅱ) ions are crystallographically equivalent and have the same coordination spheres, which is six coordinated by one nitrogen atom (N1a), five oxygen atoms (O1, O2, O2a, O2b, O3a) from the $(L^2)^{2-}$ units, and all are in distorted $[CuN_1O_5]$ octahedral geometries. Observed Cu-N bond distances lie in the normal range of 0.195 1(2) nm. The equatorial Cu-O bonds at each Cu center are shorter (ranging from 0.194 5(2) to 0.198 5(2) nm) than the axial Cu-O bond (in a range of 0.234 7(2)~0.268 2(2) nm)[52]. The metal-metal intramolecular bond distances range from 0.325 69(6) to 0.359 12(9) nm.

2.2 Supramolecular interaction of complexes 1 and 2

The intra- and intermolecular interactions data of complexes **1** and **2** are shown in Table 3 and 4. The structure of complex **1** was stabilized by three intramolecular hydrogen bonds of O5–H5C⋯O6, C15–H15⋯O3, C10–H10⋯O2 (Fig.4). An intermolecular hydrogen bonds O5–H5B⋯O2 (Fig.5) and an intermolecular non-classical C5–H5A⋯$\pi_{centroid(C11\text{-}C16)}$ interactions (Fig.6) link complex **1** molecules to form an infinite 1D supramolecular chain. Synchronously, this linkage is further stabilized via the intermolecular $\pi_{centroid(C1\text{-}C6)}\cdots\pi_{centroid(C11\text{-}C16)}$ stacking interactions between the benzene ring of adjacent complex **1** molecules with

Table 3　Putative hydrogen-bonding interactions for complexes 1 and 2

D–H⋯A	*d*(D-H) / nm	*d*(H⋯A) / nm	*d*(D⋯A)/ nm	∠(D–H⋯A) / (°)
		1		
O5–H5C⋯O6a	0.082	0.213	0.291 1(3)	158
C10–H10⋯O2	0.093	0.220	0.285 6(4)	127
C15–H15⋯O3a	0.093	0.223	0.310 6(4)	156
O5–H5B⋯O2a	0.086	0.183	0.267 9(3)	172
C5–H5A⋯Cg1a	0.298	0.294	0.336 9(4)	107
		2		
C8–H8⋯O5	0.93	2.17	2.856(3)	130

Symmetry code: 1–*x*, 2–*y*, 1–*z*; Cg1 is the centroids of C11~C16 in benzene ring.

Table 4　$\pi\cdots\pi$ stacking interactions for complexes 1 and 2

Ring (*I*)	Ring (*J*)	*d*(Cg⋯Cg) / nm	α / (°)	*d*(Cg(*I*)-perp) / nm	*d*(Cg(*J*)-perp) / nm	Slippage / nm
			1			
Cg2	Cg1a	0.428 1(2)	26.58(2)	0.283 5(1)	0.394 4(1)	0.961 0
			2			
Cg3	Cg4a	0.329 8(2)	13.77(1)	0.275 51(8)	0.307 81(9)	0.118 3
Cg3	Cg5b	0.329 8(2)	13.77(1)	0.275 51(8)	0.307 81(9)	0.118 3
Cg4	Cg6b	0.357 3(2)	13.08(9)	0.300 81(9)	0.309 50(8)	0.178 5
Cg4	Cg7c	0.357 3(2)	13.08(9)	0.300 81(9)	0.309 50(8)	0.178 5
Cg5	Cg6a	0.357 3(2)	13.08(9)	0.300 81(9)	0.309 50(8)	0.178 5
Cg5	Cg7b	0.357 3(2)	13.08(9)	0.300 81(9)	0.309 50(8)	0.178 5
Cg7	Cg6a	0.312 5(1)	15.47(8)	0.303 72(8)	0.303 71(8)	0.073 7
Cg6	Cg7b	0.312 5(1)	15.47(8)	0.303 72(8)	0.303 71(8)	0.073 7

Symmetry codes: a: 1–*x*, 2–*y*, 1–*z* for **1**; a: 3/4–*y*, 3/4+*x*, 3/4–*z*; b: –*x*, 3/2–*y*, *z*; c: –3/4+*y*, 3/4–*x*, 3/4–*z* for **2**; α=dihedral angle between planes *I* and *J*; *d*(Cg⋯Cg)=distance between ring centroids; *d*(Cg(*I*)-perp)=perpendicular distance of Cg(*I*) on ring *J*; *d*(Cg(*J*)-perp)= perpendicular distance of Cg(*J*) on ring *I*; Slippage=distance between Cg(*I*) and perpendicular projection of Cg(*J*) on ring *I*; Cg1, Cg2 are the centroids of C11~C16 and C1~C6 in benzene ring, respectively; Cg3, Cg4, Cg5, Cg6, Cg7 are the centroids of ring Cu1-O1-C2-C7-O2, Cu1a-O3c-C10c-C9c-N1c, O3-C10-C9-N1-Cu1b, Cu1-O2a-C7a-C6a-C8a-N1a and O2b-C7b-C6b-C8b-N1b-Cu1c, respectively.

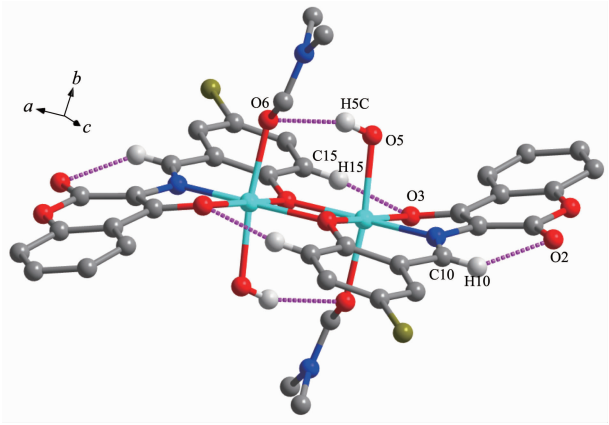

Hydrogen atoms, except those forming hydrogen bonds, are omitted for clarity

Fig.4 Intramolecular hydrogen bonding of complex **1**

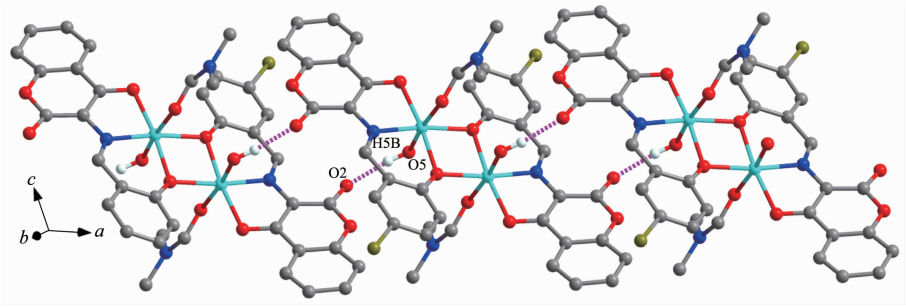

Hydrogen atoms, except those forming hydrogen bonds, are omitted for clarity

Fig.5 Intermolecular hydrogen bonding of complex **1**

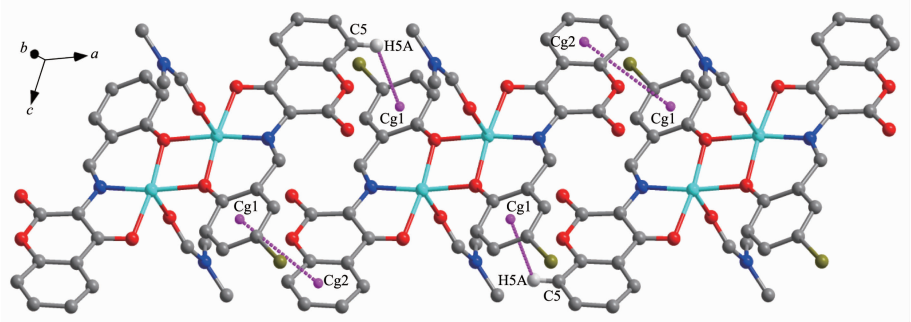

Fig.6 View of 1D supramolecular chain linked by C–H···π and π···π stacking interaction of complex **1**

the distance of 0.428 1(2) nm (Fig.6)[53-57]. Consequently, the intermolecular classical and non-classical hydrogen-bonding and $\pi \cdots \pi$ stacking interactions plays a very important role in the construction of supramolecular networks structure[58-64].

In complex **2**, the structure were only stabilized by an intramolecular non-classical hydrogen bonds of C8–H8···O5 (Fig.7 and Table 3), but there are eight complicated intermolecular $\pi \cdots \pi$ stacking interactions (Cg3···Cg4a, Cg3···Cg5b, Cg4···Cg6b, Cg4···Cg7c, Cg5···Cg6a, Cg5···Cg7b, Cg7···Cg6a, Cg6···Cg7b), with the distance of 0.329 7(7), 0.329 7(7), 0.357 3(11), 0.357 3(11), 0.357 3(0), 0.357 3(0), 0.312 5(4), 0.312 54(4) nm, respectively, which linked the neighboring molecules into a 3D network supramolecular structure (Table 4).

2.3 IR spectra analyses

The FT-IR spectra of H_2L^1, H_2L^2, and their corresponding complexes **1** and **2** exhibited various bands in the 400~4 000 cm^{-1} region, and the most

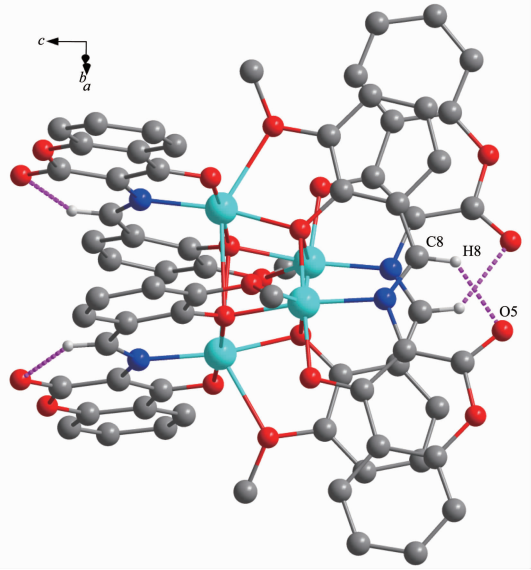

Hydrogen atoms, except those forming hydrogen bonds, are omitted for clarity

Fig.7　Intramolecular hydrogen bonding of complex **2**

important FT-IR bands for H_2L^1, complex **1** and H_2L^2, complex **2** are given in Table 5. The free ligand H_2L^1 and H_2L^2 exhibited characteristic stretching bands of C=N group at 1 670 and 1 676 cm^{-1}, respectively[65-73], while that of their corresponding complexes **1** and **2** were observed at 1 610 and 1 682 cm^{-1}, respectively. Compared with the ligand, the C =N stretching frequency of complex **1** shifted to a lower frequency by ca. 60 cm^{-1}, while that of complex **2** shifted to a higher frequency by *ca.* 6 cm^{-1}. It is indicated that the C=N bond sequence is decreased or increased due to the coordination bond between the metal atom and the imino nitrogen lone pair[74-76]. In addition, the broad O-H group stretching bands at 3 403 and 3 438 cm^{-1} for the free ligands H_2L^1 and H_2L^2, disappeared for complexes **1** and **2**, indicating the oxygen atoms in the phenolic hydroxyl groups were completely deprotonated and coordinated to the metal ions. Whereas, the stretching bands at 3 409 and 3 476 cm^{-1} in complexes **1** and **2** are attributed to the stretching vibrations of the O-H group of coordinated water or methanol. The Ar-O stretching bands at 1 230 and 1 229 cm^{-1} of complexes **1** and **2** shifted toward lower frequencies by *ca.* 35 and 12 cm^{-1}, respectively, compared with that of the free ligands H_2L^1 and H_2L^2 at 1 265 and 1 241 cm^{-1}, respectively. The lower frequency of the Ar-O stretching shift indicates that M-O bond is formed between the metal ions and the oxygen atoms of the phenolic groups[77]. The FT-IR spectrum of complex **1** showed ν(M-N) and ν(M-O) vibration frequencies at 514 and 467 cm^{-1} (or 538 and 467 cm^{-1} for complex **2**), respectively. These assignments are consistent with the frequency values in literature[78].

Table 5　Main bands in IR spectra of H_2L^1, H_2L^2 and complexes 1 and 2

cm^{-1}

Compound	ν(O-H)	ν(C=N)	ν(Ar-O)	ν(M-N)	ν(M-O)
H_2L^1	3 403	1 670	1 265	—	—
$[Ni(L1)(DMF)(H_2O)]_2$ (**1**)	3 409	1 610	1 230	514	467
H_2L^2	3 438	1 676	1 241	—	—
$[Cu_4(L_2)_4]\cdot DMF\cdot CH_3OH\cdot 2H_2O$ (**2**)	3 476	1 682	1 229	538	467

2.4　UV-Vis absorption spectra analyses

The absorption spectra of ligands H_2L^1, H_2L^2 and their corresponding Ni(Ⅱ) and Cu(Ⅱ) complexes **1** and **2** were determined in diluted DMSO solution, respectively. As shown in Fig.8, compared with complex **1**, an important feature of the absorption spectrum of H_2L^1 is shown that three absorption peaks were observed at 445, 469, 498 nm attributed to the intra-ligand π-π* transition of the C=N bonds and the conjugated aromatic chromophore, in which the absorption peak at 498 nm was absent in the spectrum of complex **1**. The absorption peaks at 445, 469 nm were blue-shifted by 2 nm and red-shifted 2 nm, respectively, indicating that Ni(Ⅱ) ion coordinates with the O and N atoms of the deprotonated ligand units. And the absorption peak at 349 nm assigned to the π-π* transitions of the phenyl rings in H_2L^1 was shifted to 351 nm in complex **1**, indicating the coordination of

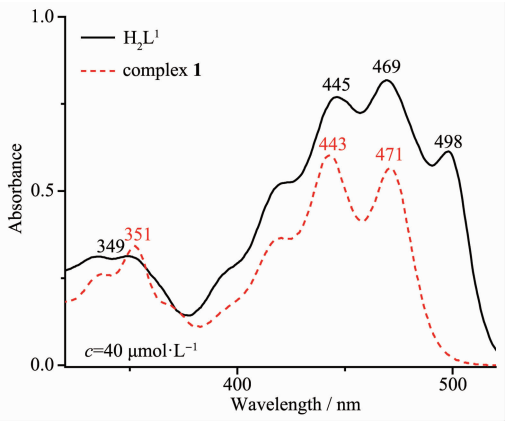

Fig.8 UV-Vis absorption spectra of H_2L^1 and complex **1** in diluted DMSO solution at room temperature

Ni(Ⅱ) atom with $(L^1)^{2-}$.

The electronic absorption spectrum of free ligand H_2L^2 exhibited three absorption peaks at approximately 389, 412 and 437 nm (Fig.9). The former absorption peaks at 389 nm can be assigned to the π-π^* transition of benzene rings and the latter at 412 and 437 nm can be attributed to the intra-ligand π-π^* transition of C=N group [79]. Upon coordination of the ligand, the absorption peaks at 412 and 437 nm were red-shifted to 416 and 438 nm, respectively, indicating that the amino nitrogen is involved in coordination with Cu(Ⅱ) ion[80]. The intraligand π-π^* transitions of the benzene ring were bathochromically shifted to 343 and 360 nm in complex **2**, indicating the coordination of Cu(Ⅱ) ion with deprotonated $(L^2)^{2-}$ unit.

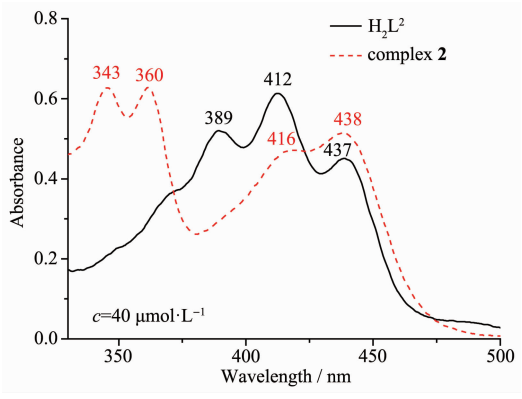

Fig.9 UV-Vis absorption spectra of H_2L^2 and complex **2** in diluted DMSO solution at room temperature

2.5 Emission spectra of complexes 1 and 2

The fluorescence emission spectra of the ligands H_2L^1, H_2L^2 and their corresponding Ni(Ⅱ) and Cu(Ⅱ) complexes **1** and **2** were determined at room temperature in a diluted DMSO solution. As shown in Fig. 10, the free ligand H_2L^1 showed stronger fluorescence emission at 413, 439 and 518 nm with the excitation at 370 nm, respectively, which could be assigned to the intraligand π^*-π transition. Compared with H_2L^1, the emission peaks of complex **1** was slightly blue-shifted 1~2 nm, and the fluorescence intensity at 412, 437 nm tended to increase and that at 518 nm tended to decrease significantly, indicating that the Ni(Ⅱ) ion coordinates with the N and O atoms and electron transition occurs.

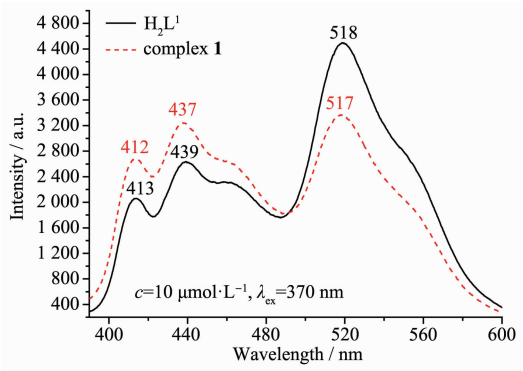

Fig.10 Emission spectra of H_2L^1 and complex **1** in diluted DMSO at room temperature

Meanwhile, the ligand H_2L^2 exhibited a relatively strong emission peak at *ca.* 507 nm and a weaker emission peak at 414 nm upon excitation at 370 nm (Fig.11), which could be assigned to the intraligand π^*-π transition. Compared with the H_2L^2, the emission intensity at 507 nm reduced obviously and that at 414 nm tended to increase for complex **2**, indicating that the Cu(Ⅱ) ion coordinates with the N and O atoms and electron transition occurs. The fluorescence intensity

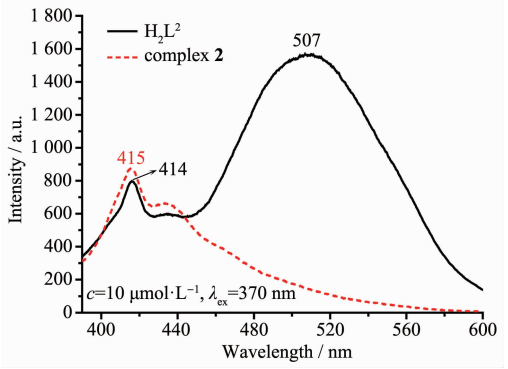

Fig.11 Emission spectra of H_2L^2 and complex **2** in diluted DMSO at room temperature

of the free ligands H_2L^2 is probably enhanced via the occurrence of a photoinduced electron transfer process owing to the presence of a lone pair of nitrogen atoms. The process is prevented by the complexation of the free ligand H_2L^2 with the Cu(Ⅱ) ions. Therefore, the coordination of Cu(Ⅱ) ions can effectively reduce the fluorescence intensities[81].

3 Conclusions

Based on two Schiff base ligands, dinuclear complex **1** and cubane-like $Cu_4(\mu_3\text{-}O)_4$ core tetranuclear complex **2** were synthesized and their structural characterization and fluorescence properties were carried out. The crystal structure analysis of complexes **1** and **2** shows that the atomic configurations of Ni(Ⅱ) and Cu(Ⅱ) are all six-coordinated distorted octahedrons. Complex **1** self-assembles into a 1D supramolecular chain through intermolecular hydrogen bonding, C–H $\cdots\pi$ and $\pi\cdots\pi$ stacking interactions, and complex **2** self-assembles into a 3D supramolecular network structure through intramolecular hydrogen bonding and $\pi\cdots\pi$ stacking interactions. Furthermore, the optical properties of complexes **1** and **2** indicate that the fluorescence variation of H_2L^1 and H_2L^2 is due to the coordination of the metal ions Ni(Ⅱ) and Cu(Ⅱ).

References:

[1] Liu Y A, Wang C Y, Zhang M, et al. *Polyhedron*, **2017**,**127**: 278-286

[2] Dong W K, Ma J C, Dong Y J, et al. *Polyhedron*, **2016**,**115**: 228-235

[3] Dong W K, Bai Y, Zhang L S, et al. *Asian J. Chem*., **2014**, **26**:2341-2343

[4] Sun Y X, Zhang S T, Ren Z L, et al. *Synth. React. Inorg. Met.-Org. Nano-Met. Chem.*, **2013**,**43**:995-1000

[5] YANG Yu-Hua(杨玉华), HAO Jing(郝静), DONG Yin-Juan (董银娟), et al. *Chinese J. Inorg. Chem.*(无机化学学报), **2017**,**33**:1280-1292

[6] Wu H L, Pan G L, Bai Y C, et al. *J. Chem. Res.*, **2014**,**38**: 211-217

[7] Wu H L, Yuan J K, Bai Y, et al. *Dalton Trans.*, **2012**,**41**: 8829-8838

[8] Li X Y, Kang Q P, Liu L Z, et al. *Crystals*, **2018**,**8**:43

[9] Wu H L, Pan G L, Bai Y C, et al. *Res. Chem. Intermed.*, **2015**,**41**:3375-3388

[10]Chen C Y, Zhang J W, Zhang Y H, et al. *J. Coord. Chem.*, **2015**,**68**:1054-1071

[11]Wu H L, Bai Y H, Zhang Y H, et al. *Z. Anorg. Allg. Chem.*, **2014**,**640**:2062-2071

[12]Hao J, Li L L, Zhang J T, et al. *Polyhedron*, **2017**,**134**:1-10

[13]Wu H L, Wang C P, Wang F, et al. *J. Chin. Chem. Soc.*, **2015**,**62**:1028-1034

[14]Song X Q, Liu P P, Xiao Z R, et al. *Inorg. Chim. Acta*, **2015**, **438**:232-244

[15]Dong W K, Li X L, Wang L, et al. *Sens. Actuators B*, **2016**, **229**:370-378

[16]Liu P P, Sheng L, Song X Q, et al. *Inorg. Chim. Acta*, **2015**, **434**:252-257

[17]Dong W K, Ma J C, Zhu L C, et al. *New J. Chem.*, **2016**,**40**: 6998-7010

[18]Zhang H, Dong W K, Zhang Y, et al. *Polyhedron*, **2017**,**133**: 279-293

[19]Dong X Y, Akogun S F, Zhou W M, et al. *J. Chin. Chem. Soc.*, **2017**,**64**:412-419

[20]Li X Y, Kang Q P, Liu C, et al. *New J. Chem.*, **2019**,**43**: 4605-4619

[21]Dong Y J, Dong X Y, Dong W K, et al. *Polyhedron*, **2017**, **123**:305-315

[22]Li G, Hao J, Liu L Z, et al. *Crystals*, **2017**,**7**:217

[23]Liu L Z, Wang L, Yu M, et al. *Spectrochim. Acta Part A*, **2019**,**222**:117-209

[24]Kang Q P, Li X Y, Wang L, et al. *Appl. Organomet. Chem.*, **2019**:e5013

[25]Chai L Q, Tang L J, Chen L C, et al. *Polyhedron*, **2017**,**122**: 228-240

[26]Chai L Q, Zhang K Y, Tang L J, et al. *Polyhedron*, **2017**, **130**:100-107

[27]Chen L, Dong W K, Zhang H, et al. *Cryst. Growth Des.*, **2017**,**17**:3636-3648

[28]LU Rui-E(陆瑞娥), LI Xin-Ran(李新然), ZHAO Ya-Yuan (赵亚元), et al. *Chinese J. Inog. Chem.*(无机化学学报), **2015**,**31**:1055-1062

[29]Wang P, Zhao L. *Synth. React. Inorg. Met.-Org. Nano-Met. Chem.*, **2016**,**46**:1095-1101

[30]Zhao L, Dang X T, Chen Q, et al. *Synth. React. Inorg. Met.-Org. Nano-Met. Chem.*, **2013**,**43**:1241-1246

[31]Sun Y X, Wang L, Dong X Y, et al. *Synth. React. Inorg. Met.-Org. Nano-Met. Chem.*, **2013**,**43**:599-603

[32]Dong W K, Ma J C, Zhu L C, et al. *Cryst. Growth Des.*, **2016**,**16**:6903-6915

[33]DONG Wen-Kui(董文魁), WANG Li(王莉), SUN Yin-Xia (孙银霞), et al. *Chinese J. Inorg. Chem.*(无机化学学报),

2011,**27**:372-376

[34]Wu H L, Peng H P, Zhang Y H, et al. *Appl. Organomet. Chem.*, **2015**,**29**:443-449

[35]LIU Ling-Zhi(刘玲芝), YU Meng(于萌), LI Xiao-Yan(李肖研), et al. *Chinese J. Inorg. Chem.*(无机化学学报), **2019**, **35**:1283-1294

[36]SUN Yin-Xia(孙银霞), LI Chun-Yu(李春宇), YANG Cheng-Juan(杨成娟), et al. *Chinese J. Inorg. Chem.*(无机化学学报), **2016**,**32**:327-335

[37]Dong W K, Zhu L C, Ma J C, et al. *Inorg. Chim. Acta*, **2016**,**453**:402-408

[38]YANG Yu-Hua(杨玉华), HAO Jing(郝静), DONG Yin-Juan(董银娟), et al. *Chinese J. Inorg. Chem.*(无机化学学报), **2017**,**33**:1280-1292

[39]Sun Y X, Gao X H. *Synth. React. Inorg. Met.-Org. Nano-Met. Chem.*, **2011**,**41**:973-978

[40]Kang Q P, Li X Y, Wei Z L, et al. *Polyhedron*, **2019**,**165**: 38-50

[41]Li L H, Dong W K, Zhang Y, et al. A*ppl. Organomet. Chem.*, **2017**,**31**:e3818

[42]Li X Y, Chen L, Gao L, et al. *RSC Adv.*, **2017**,**7**:35905-35916

[43]Zhao Q, An X X, Liu L Z, et al. *Inorg. Chim. Acta*, **2019**, **490**:6-15

[44]Hu J H, Sun Y, Qi J, et al. *Spectrochim. Acta Part A*, **2017**, **175**:125-133

[45]An X X, Zhao Qi, Mu H R, et al. *Crystals*, **2019**,**9**:101

[46]Wu H L, Bai Y C, Zhang Y H, et al. *J. Coord. Chem.*, **2014**, **67**:3054-3066

[47]Wu H L, Pan G L, Bai Y C, et al. *J. Coord. Chem.*, **2013**, **66**:2634-2646

[48]Danis O, Yuce-Dursun B, Gunduz C, et al. *Arzneim.-Forsch.*, **2010**,**60**:617-620

[49]*SAINT-Plus, Ver.* 6.02, Bruker Analytical X-ray System, Madison, WI, **1999**.

[50]Sheldrick G M. *SADABS, Program for Empirical Absorption Correction of Area Detector Data*, University of Göttingen, Germany, **1996**.

[51]Sheldrick G M. *SHELXS*-97, *Program for the Solution and the Refinement of Crystal Structures*, University of Göttingen, Germany, **1997**.

[52]Wang F, Liu L Z, Gao L, et al. *Spectrochim. Acta Part A*, **2018**,**203**:56-64

[53]Dong W K, Wang Z K, Li G, et al. *Z. Anorg. Allg. Chem.*, **2013**,**639**:2263-2268

[54]Chai L Q, Huang J J, Zhang J Y, et al. *J. Coord. Chem.*, **2015**,**68**:1224-1237

[55]Wang P, Zhao L. *Asian J. Chem.*, **2015**,**4**:1424-1426

[56]Chai L Q, Wang G, Sun Y X, et al. *J. Coord. Chem.*, **2012**, **65**:1621-1631

[57]Wu H L, Bai Y, Yuan J K, et al. *J. Coord. Chem.*, **2012**,**65**: 2839-2851

[58]Dong W K, Zhang X Y, Sun Y X, et al. *Synth. React. Inorg. Met.-Org. Nano-Met. Chem.*, **2015**,**45**:956-962

[59]Dong Y J, Li X L, Zhang Y, et al. *Supramol. Chem.*, **2017**, **29**:518-527

[60]Wang B J, Dong W K, Zhang Y, et al. *Sens. Actuators B*, **2017**,**247**:254-264

[61]Wang L, Hao J, Zhai L X, et al. *Crystals*, **2017**,**7**:277

[62]Ma J C, Dong X Y, Dong W K, et al. *J. Coord. Chem.*, **2016**,**69**:149-159

[63]Dong W K, Zhu L C, Dong Y J, et al. *Polyhedron*, **2016**,**117**: 148-154

[64]Xu L, Zhu L C, Ma J C, et al. *Z. Anorg. Allg. Chem.*, **2015**, **641**:2520-2524

[65]Wu H L, Pan G L, Bai Y C, et al. *J. Photochem. Photobiol. B*, **2014**,**135**:33-43

[66]Song X Q, Peng Y J, Chen G Q, et al. *Inorg. Chim. Acta*, **2015**,**427**:13-21

[67]Hu J H, Li J B, Qi J, et al. *New J. Chem.*, **2015**,**39**:843-848

[68]Liu P P, Wang C Y, Zhang M, et al. *Polyhedron*, **2017**,**129**: 133-140

[69]Chai L Q, Zhang H S, Huang J J, et al. *Spectrochim. Acta Part A*, **2015**,**137**:661-669

[70]Dong W K, Zhang F, Li N. *Z. Anorg. Allg. Chem.*, **2016**, **642**:532-538

[71]Wang P, Zhao L. *Spectrochim. Acta. Part A*, **2015**,**135**:342-350

[72]Gao L, Wang F, Zhao Q, et al. *Polyhedron*, **2018**,**139**:7-16

[73]Dong W K, Ma J C, Dong Y J, et al. *J. Coord. Chem.*, **2016**, **69**:3231-3241

[74]Wu H L, Huang X C, Yuan J K, et al. *Z. Naturforsch.*, **2011**, **66b**:1049-1055

[75]Wu H L, Li K, Sun T, et al. *Transition Met. Chem.*, **2011**, **36**:21-28

[76]Wu H L, Wang K T, Kou F, et al. *J. Coord. Chem.*, **2010**, **64**:2676-2687

[77]Sun Y X, Xu L, Zhao T H, et al. *Synth. React. Inorg. Met.-Org. Nano-Met. Chem.*, **2013**,**43**:509-513

[78]Sun Y X, Wang L, Dong X Y, et al. *Synth. React. Inorg. Met.-Org. Nano-Met. Chem.*, **2013**,**43**:599-603

[79]Zhang Y G, Shi Z H, Yang L Z, et al. *Inorg. Chem. Commun.*, **2014**,**39**:86-89

[80]Wang F, Gao L, Zhao Q, et al. *Spectrochim. Acta Part A*, **2018**,**190**:111-115

[81]Chai L Q, Mao K H, Zhang J Y, et al. *Inorg. Chim. Acta*, **2017**,**457**:34-40